Electronic band structure of $Al_xGa_{1-x}As/Al_yGa_{1-y}As/GaAs$ double-barrier superlattices

T. Osotchan, V. W. L. Chin, M. R. Vaughan, T. L. Tansley, and E. M. Goldys
Semiconductor Science and Technology Laboratories, Physics Department, Macquarie University, New South Wales 2109, Australia
(Received 4 March 1994; revised manuscript received 28 April 1994)

The results of a semiempirical tight-binding calculation of conduction bands in (001) $Al_xGa_{1-x}As/Al_yGa_{1-y}As/GaAs$ double-barrier superlattices are described. The parameters chosen are appropriate to the design of an $Al_{0.3}Ga_{0.7}As/AlAs/GaAs$ structure for quantum-well infrared-photodetector (QWIP) applications in the 3–5-μm band. The dependence of the superlattice conduction-band energy levels on slab thicknesses, alloy compositions, and wave vector are examined. The tight-binding method has the ability to describe states far away from the center of the Brillouin zone and band mixing is shown in the characteristic energy-dependence curves. States can be identified as Γ-valley-like or X-valley-like, due to Γ or X electron localization in the wells formed by the GaAs, $Al_yGa_{1-y}As$, or $Al_xGa_{1-x}As$ slabs. The Γ-valley-like states of GaAs wells in the $Al_{0.3}Ga_{0.7}As/AlAs/GaAs$ structure (the transition states for QWIP applications) have energies close to those of a simple AlAs/GaAs square superlattice when the number of AlAs layers is greater than 4. In addition to the GaAs well states, the results show that the X-valley-like bound states from the surrounding AlAs slabs consist of two closely spaced energy eigenvalues, the doublet splits when the two AlAs slabs become closer as the thickness of the intervening GaAs (or $Al_{0.3}Ga_{0.7}As$) slab is reduced. Band mixing is evident from the results obtained by varying the Al mol fraction of $Al_yGa_{1-y}As$ or $Al_xGa_{1-x}As$ barriers. Crossing and anticrossing behavior is noted at specific compositions x and y where states interfere. The energy-dispersive relations along wave vectors parallel to the interface have also been calculated. Curvatures differ due to the different effective masses of Γ-valley- and X-valley-like states.

I. INTRODUCTION

The electronic energy levels associated with semiconductor superlattices (SL) can be tailored by adjusting the alloy compositions or doping concentrations or both and by selection of individual thicknesses of the homogeneous semiconductor slabs constituting the SL. Engineering at the monolayer level is particularly accessible in the $Al_xGa_{1-x}As$ ternary system through relatively simple growth by molecular-beam epitaxy (MBE). Recently, there has been a great interest in the design and use of $Al_xGa_{1-x}As/GaAs$ heterostructures as quantum-well infrared photodetectors (QWIP).[1–5] In general terms, the QWIP is designed so that individual wells confine two bound-electron states, broadened into two minibands when assembled into a short-period SL. Figure 1(a) shows schematically (solid lines only) the band-edge profiles and carrier minibands in such a structure. At intermediate periodicity, essentially only the upper state forms a band while the lower remains bound. A doping regime is chosen so that lower and upper levels are full and empty, respectively, and photoexcitation between them becomes possible. Excited electrons extracted into the conduction-band continuum may then be observed as a photocurrent in an external circuit. Extraction through thermal excitation into the continuum competes with thermal relaxation into the lower levels, but can be enhanced by applying a sufficiently large bias voltage for excited electrons to tunnel out. Excessively large voltage, however, can cause undesirable leakage from the heavily-populated lower state. The excited state is therefore usually chosen to lie close to the top of the well. In order to overcome some of these difficulties, interest has recently shifted towards studies of excitations from bound to extended-continuum states,[1,6,7] bound states to minibands,[8,9] or bound states to extended-quasi-bound states.[1,10–13] The extended-quasi-bound state can be induced by adding a further thin barrier to each side of the well as shown schematically in the double barrier (DB) profile of Fig. 1(b). This modification also results in increased absorption peak energy[10,11] and responsitivity of the device.[12,13] The $Al_xGa_{1-x}As/Al_yGa_{1-y}As/GaAs$ DB system can thus be designed as an effective infrared photodetector of shorter wavelengths in the 3–5 μm regime.[10–12] Moreover, the bandwidth of the responsitivity spectrum can also be controlled in such DB structures.[1,13]

Narrowing the GaAs well and increasing the aluminum content in the $Al_xGa_{1-x}As$ barrier increases the transition energy between two bound states and shortens the response wavelength of the detector. At compositions above $x=0.45$, $Al_xGa_{1-x}As$ becomes indirect gap and the minimum operating wavelength obtainable by simple square-well bound-to-bound-state transitions is approximately 5.6 μm.[14] However, adding thin barriers of $Al_yGa_{1-y}As$ to both sides of the GaAs well shifts the excited electron energy in the well towards higher energy[10,11,15,16] without introducing a full-width indirect-gap barrier between adjacent wells. This is important because the conduction–band satellite minima are significantly lower than the zone-center minimum in the alloys of high AlAs content.

In a simple $Al_xGa_{1-x}As/GaAs$ SL with $x<0.45$, both wells and barriers are direct-gap semiconductors with

conduction-band minimum in the Γ valley. The band-edge profiles therefore correspond to a type-I SL, with electrons and holes confined in the same layer of the structure, in this case the GaAs well. However, in AlAs/GaAs SL built in (001) orientation, type-II structures can occur as follows. Using parameters from Ref. 17, the conduction-band edge of GaAs at $k_x = 2\pi/a$ (X_c) is 1.916 eV above the Γ_v valence-band edge while Γ_c is 1.430 eV above. In AlAs the corresponding values are 2.026 eV for X_c and 3.002 eV for Γ_c. However, at heterointerfaces between GaAs and AlAs (and intermediate ternaries) approximately 32% (Refs. 18–22) of the band-gap discontinuity, or 0.5 eV, appears as a step in Γ_v. Thus X_c, measured from the valence-band edge of GaAs, falls by 0.390 eV in the transition from GaAs to AlAs and this is shown as the dashed line in Fig. 1(a). Electrons in X minima are relatively heavy and it is possible to arrange GaAs and AlAs slab thicknesses so that confined states in the latter are at lower energies than those in the former, as also indicated in Fig. 1(a). This

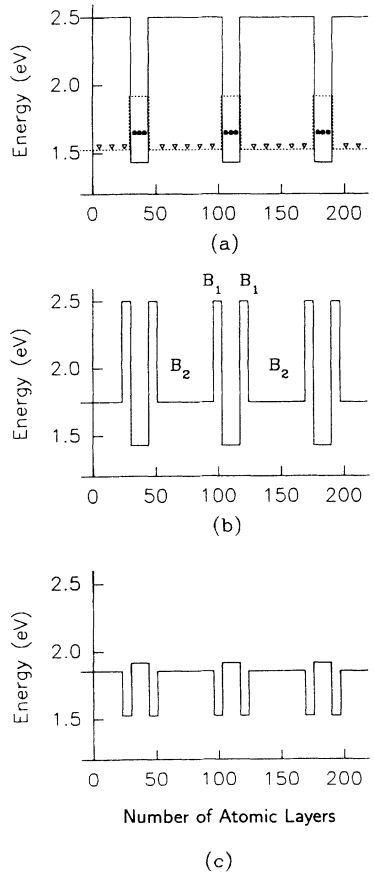

FIG. 1. Schematic of typical CB edge profiles (a) for a simple GaAs/AlAs superlattice, solid and broken lines locate Γ and X minima, respectively, with the Γ-like well in GaAs and the X-like wells in AlAs. Filled circle shows possible confined states in GaAs, triangle for a state in AlAs which, as shown, may be the lowest-energy confined state, (b) and (c) represent the CB edge profiles for $Al_{0.3}Ga_{0.7}As/AlAs/GaAs$ SL, at Γ minima ($k_x = 0$) and X point ($k_x = 2\pi/a$), respectively.

constitutes, through the intervention of the X minimum, a type-II SL with electrons and holes confined in the different media and has been shown to occur for GaAs layers less than 3.5 nm thick combined with AlAs thicker than 1.5 nm.[23] The contribution of satellite minima clearly cannot be ignored in $Al_xGa_{1-x}As/Al_yGa_{1-y}As/GaAs$ DBSL in certain ranges of aluminum content and slab thickness.

As an additional parameter, external hydrostatic pressure can be applied to drive the Γ-valley states in type-I SL to relatively higher energy than X-valley counterparts, forming a type-II SL. Recently, the confined electron energies in ultrathin single QWDB AlAs have been measured under pressure and an envelope-function approximation has been used in their calculation.[24]

The Kronig-Penney or envelope-function-matching (EFM) approximation[25] is a simple and useful method which is adequate for SL state calculations where there is only one dominating bulk state in each material. If two or more bulk states with widely separated wave vectors contribute significantly to a given SL state, the one band EFM approximation will not automatically account for this effect. The $Al_xGa_{1-x}As/Al_yGa_{1-y}As/GaAs$ SL state across a full range of Al mol fractions evolves from a mixture of Γ and X like states. The tight-binding method has the ability to describe the band structure far away from the center of the Brillouin zone and it is the obvious candidate for a range of problems in band mixing.[17,26–32] In the conventional tight-binding method, the energies at the high-symmetry points are used to fix the tight-binding parameters. However, for sp^3, this model yields larger than experimental effective masses in the Γ and X valleys and high conduction X-minima energy. A number of efforts, such as addition of an excited s^* or d state to the sp^3 model, and/or including second-neighbor interactions,[27,32] have been made to bring effective masses and the X minima closer to the experimental values. Nevertheless, in order to carry out such a calculation while still showing the effects of states far from symmetry points and including band mixing, we have opted to use an sp^3s^* model with the first-nearest-neighbor interaction.[17,26,28–31] The conduction-band SL energy levels obtained are expected to result in a slight shift in an absolute energy compared to methods such as EFM which use the exact parameters at the critical points.

We have used the semiempirical tight-binding method to calculate the electron band structure for (001) $Al_xG_{1-x}As/Al_yGa_{1-y}As/GaAs$ DB structure by varying a range of parameters including structural dimensions and alloy compositions. Our approach is to study the energy levels in the conduction subband of the DB structure in general and to discuss in particular the band mixing effects appearing in these levels. In Sec. II, the tight-binding model is briefly reviewed and its application to the DB structure is described in detail. Our results for the (001) $Al_xGa_{1-x}As/Al_yGa_{1-y}As/GaAs$ DBSL are discussed in Sec. III. The dependence of SL conduction bands on slab thickness, alloy composition and wave-vector components in the plane of the structure are also addressed in Sec. III.

II. CALCULATION METHOD

A. Tight-binding approach

A semiempirical tight-binding Hamiltonian (sp^3s^*) was used with nearest-neighbor interactions, including excited anion (As) and cation (Al and Ga) s^* states, included with in the normal s,p_x,p_y,p_z basis. The excited s^* state allows the lowest bulk conduction-band near X minima to be fitted well. The SL state is then expanded in terms of ten semiconductor bulk states of the material in each layer.

$$\Psi_{\mathbf{k},\mathbf{q}}(\mathbf{r}) = \sum_L e^{iqL} \sum_{\sigma=1}^{4} \sum_{m_\sigma} \sum_{n=1}^{10} C_n^{(\sigma)} \sum_l e^{i\mathbf{k}\cdot\boldsymbol{\rho}_l} \varphi_n^{(\sigma)}(\mathbf{r}-\boldsymbol{\rho}_l - L\mathbf{z}) ,$$

where $\varphi_n^{(\sigma)}$ is the bulk state of the material with bulk quantum number $n=1-10$ and slab material index $\sigma=1-4$. These bulk states have been written in the form of hybridized orbitals directed along the bond directions for convenience of the superlattice calculation in different directions of crystal growth.[33] Here z is the direction perpendicular to the interfaces, ρ_l is a lattice vector parallel to the interface, $\mathbf{q}$ is the SL wave vector in the z direction, $\mathbf{k}=(k_x,k_y)$ is a two-dimensional wave vector parallel to the interface, L denotes the SL unit-cell position, and the $C_n^{(\sigma)}$ are the expansion coefficients of the bulk states. The exponential terms $e^{i\mathbf{k}\cdot\boldsymbol{\rho}}$ and e^{iqL} are the respective Bloch function periodicities of the atomic arrangement along the interface plane and of the SL unit cell along the z axis. The summation over m_σ is to account for all the number of the atomic layers in each SL slab of index σ. Let $m_1,\ldots,m_4$ represent the number of layers in the four slabs of the DB structure unit, then there will be a total of $(\Sigma m_\sigma)\times 10$ basis wave functions per unit SL cell and the Hamiltonian matrix has $[(\Sigma m_\sigma)\times 10]^2$ elements.

The semiempirical tight-binding parameters of the binary semiconductors with the sp^3s^* basis used in this calculation were as described in Ref. 17. They were adjusted in order to reproduce the characteristics of the energy bands more accurately in the vicinity of the valence and conduction-band edges, especially the effective mass which has a strong influence on the SL energy levels. Parameters of the other compositions in the $Al_xGa_{1-x}As$ alloy system were obtained by linear interpolation of the two binary semiconductor parameter sets.

The relative positions of the bands in two adjacent semiconductor layers are specified by the conduction-band offset (ΔE_c). This implies that the diagonal terms of each pair of semiconductor layers are relatively shifted. In the calculation, the energy of the GaAs valence-band maximum has been set to zero. In principle, the offset magnitude can be computed in tight binding with a reasonable precision,[34,35] we have however conformed with other workers in calculating the conduction band offset from 68% of direct band-gap difference between the two adjacent semiconductors.[18–22]

The energy and coefficients are then found by a straightforward diagonalizing of the Hamiltonian matrix[36] formed using the $\Psi_{\mathbf{k},\mathbf{q}}(\mathbf{r})$ as a basis and finally the wave function can be expressed in terms of local-orbital coefficients. In order to check our procedure, an SL consisting of two identical simple square-well units was used as a trial. These results were compared with the very precise ones obtained by Schulman and Chang.[17] Our results are in excellent agreement with those obtained from their method.

B. Parameter Setting

The electron energy states of the (001) $Al_xGa_{1-x}As/Al_yGa_{1-y}As/GaAs$ SL were calculated as functions of the number of layers and alloy compositions chosen with design device parameters for 3–5 μm QWIP applications in mind. The well width was selected to incorporate only one Γ-like bound state in the well at energies below that of the outer barrier which we have designated B_2 [see Fig. 1(b)]. The electron confined in this state would therefore not be able to tunnel through the thin barrier [B_1 of Fig. 1(a)]. For practical reasons of MBE growth, the Al mol fraction (y) in the B_1 barrier is usually 1. The Al mol fraction (x) in the B_2 barrier was initially chosen to be 0.3 to retain a direct gap. The B_1 barrier must be thin enough for the excited electron to be able to tunnel through, so two and seven layers were selected. The B_2 outer barrier acts as a spacer between adjacent DB structures, it is usually taken to be very wide so that interference between adjacent structures may be safely neglected. However, the size of the computational matrix becomes bigger when the number of layers increases, and we have not chosen to exceed 45 layers for the B_2 barrier. The control structure around which we varied parameters is thus a repetition of the pattern; 45 layers of $Al_{0.3}Ga_{0.7}As$, two or seven layers of AlAs, 14 layers of GaAs, and then two or seven layers of AlAs.

C. Band-edge profile consideration

Figures 1(b) and 1(c) show the schematic DB energy profiles for the conduction-band edge at the center of the Brillouin zone (Γ minimum) and at the X point ($\mathbf{k}=(2\pi/a,0,0)$), respectively. The actual conduction-band-edge profile is more complicated because the X minima for GaAs and $Al_xGa_{1-x}As$ alloy are not at the same point in the zone. The locations are $k_x=0.84(2\pi/a)$ and $k_x=0.79(2\pi/a)$ for GaAs and AlAs X minima, respectively.[17] Note that the conduction band edge at X point for both B_1 and B_2 is always lower than that in the GaAs. The Γ minimum, on the other hand, is always lower in the GaAs well than in either alloy. This means that the electrons near the X minima see the slabs with higher Al concentration as the wells, while electrons near the Γ minimum see the slabs with lower Al concentration as the wells. For convenience, they will be called the X-like wells and Γ-like wells, respectively.

The conduction-band-edge alignment for electrons near Γ minima, Fig. 1(b), shows a double barrier on each side of the GaAs well comprising the AlAs B_1 barrier and the $Al_xGa_{1-x}As$ B_2 barrier. Electrons with energy

greater than the conduction-band edge of B_2 see it as a shallower well enclosed by thin B_1 barriers. Since the B_1 slab is usually thin enough to support electron tunneling, the electron states from these two wells have strong interaction.

For X-like electrons, the conduction-band edge of B_1 lies at the lowest energy and the conduction-band edge of B_2 and GaAs are at higher but different energies. B_1 therefore acts as a deep but asymmetric well with different barrier heights on each side.

An important factor in determining the SL band structure is the selection of appropriate electron effective masses. For (001) superlattice in $Al_xGa_{1-x}As/GaAs$, the three important effective masses are those in the Γ valley, m_Γ, and in the X-valley m_t (transverse) and m_1 (longitudinal). The longitudinal X-band effective mass is large, the transverse X-band effective mass is smaller, and the Γ mass is even smaller.

III. RESULTS AND DISCUSSION

In our calculation, we adopted the following routine, reflected in the order of discussion in following sections. The electron energies were first calculated as a function of the number of layers in the B_1 barrier. On the basis of this result the two and seven layer thicknesses were selected as representative of the effects of barrier B_1 and each was successively fixed while the other parameters were varied. The wave function of each state was calculated to confirm electron confinement in B_1, B_2, or GaAs slabs. Second, the number of GaAs layers was varied to determine the variation of response energy possible in the structure. In order to understand electron states completely, the SL energy state as a function of Al content in both barriers B_1 and B_2 were also investigated. Finally, the dependence of energy state on the wave vector was calculated.

A. Dependence on number of layers

The number of layers, thickness of slab, or well and barrier width are significant parameters for designing the response for a given device. In the case of the double-barrier QWIP, the wavelength response is determined by the energy separation between the two subband states. However, slab thickness has other effects on device operation, the ability of an electron to travel through it, for example. We, therefore, first discuss electron energies at the zone center ($\mathbf{k}=\mathbf{0},\mathbf{q}=\mathbf{0}$) of the (001) $Al_{0.3}Ga_{0.7}As/AlAs/GaAs$ SL as a function of the number of layers in each B_1 barrier slab as shown in Fig. 2.

The Γ minimum in B_2 lies at an energy of 1.751 eV at this composition, and there are a few states at energies below this. One set has almost constant energy of about 1.590 eV and the other set has energy decreasing as the number of B_1 layers increases. The former, which lies at 1.582 eV in the specific example of two B_1 layers, has a wave function of large amplitude in the GaAs slab, as shown in frame 1 of Fig. 3. (Frame 16 shows the structure band-edge profile with the same monolayer scale.)

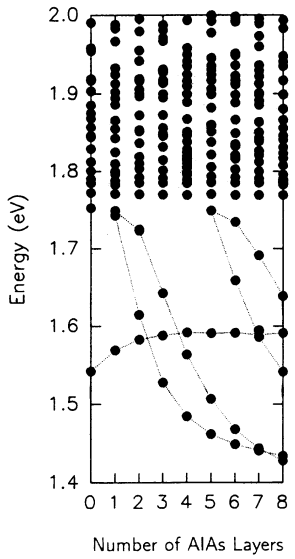

FIG. 2. Conduction-band-energy levels for $\mathbf{k}=0$, $\mathbf{q}=0$ states of the (001) $Al_{0.3}Ga_{0.7}As/AlAs/GaAs$ superlattice as a function of the number of AlAs barrier layers. The thicknesses of the $Al_{0.3}Ga_{0.7}As$ and GaAs slabs are fixed at 45 and 14 layers, respectively.

The almost-constant 1.590-eV level is therefore identified with the Γ-like bound state in the GaAs well.

As the number of B_1 layers passes 4, the Γ-like bound-state energy asymptotically approaches that of a simple GaAs square well with AlAs barriers. However, when the B_1 slab is decreased below five layers, the eigenenergy decreases slightly, even though the well width is still constant. The limiting value, where the number of B_1 layer is zero, is that of the simple well with $Al_{0.3}Ga_{0.7}As$ barriers only.

The $Al_{0.3}Ga_{0.7}As/AlAs/GaAs$ SL structure (with 14 GaAs layers), thus has only one Γ-like bound state in GaAs well with energy lower than the B_2 barrier height, as illustrated in Fig. 2. For less than three AlAs layers, this is the state of lowest energy and is of SL type-I character.

Figure 2 also shows a group of states whose energy decreases as the number of AlAs layer increases, analogous to the eigenenergy decrease in quantum wells of increasing widths. Frames 2–5 of Fig. 3 identify these as X-like bound states in the AlAs slabs. The examples shown are for four wave functions at 1.613, 1.614, 1.723, and 1.725 eV in an $Al_{0.3}Ga_{0.7}As/AlAs/GaAs$ SL structure with 2 AlAs layers. The first pair (1.613/1.614 eV, frames 2 and 3) represent AlAs X-like well bound states with a small proportion of atomic anion amplitude, while the second pair (1.723/1.725 eV, frames 4 and 5) are for a similar state with stronger anion amplitude. In each case the splitting is due to the slight interaction (because of their relatively large spatial separation) between identical states in the two AlAs slabs forming symmetric and asymmetric total wave functions.

With less than five AlAs layers, (Fig. 2) there are only two decreasing curves associated with X-like ground

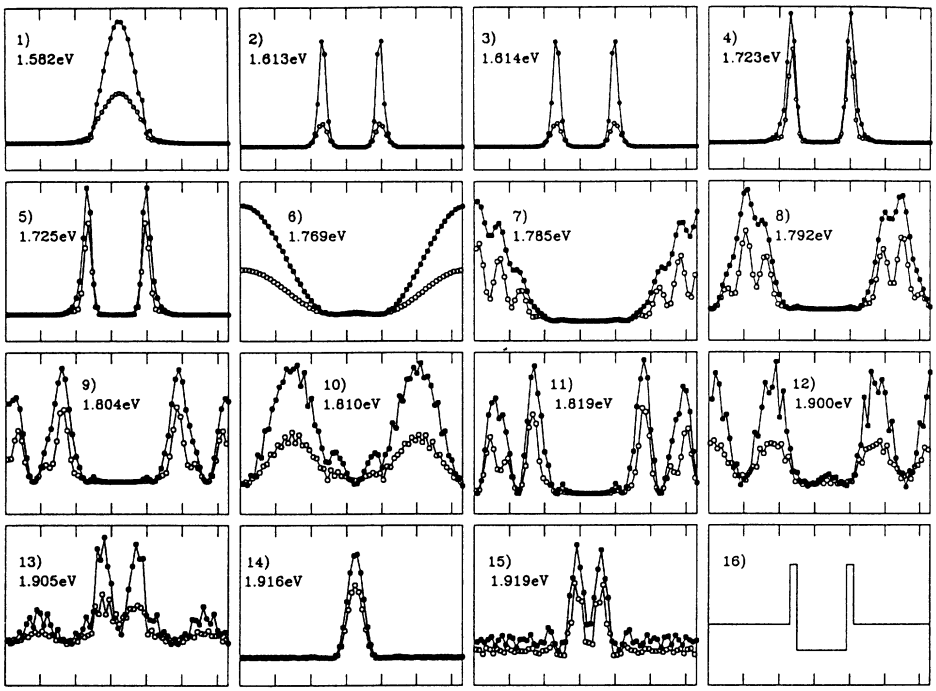

FIG. 3. Squares of wave functions for some selected zone-center states of the (001) $Al_{0.3}Ga_{0.7}As/AlAs/GaAs$ superlattice, frames 1–15, in order of increasing energy. The Γ valley conduction-band-edge profile is shown in frame 16, a vertical mark spaces every ten monolayers throughout. A filled circle represents an atomic cation layer and open circle represents an anion layer. There are 23 layers of $Al_{0.3}Ga_{0.7}As$ at left of each graph, followed by two layers of AlAs, 14 layers of GaAs, a further two layers of AlAs, and then 22 layers of $Al_{0.3}Ga_{0.7}As$.

states as their wave functions have only one node. When the number of AlAs layers is greater than five however, there are two additional decreasing curves for X bound states. These are the excited states identified by wave functions (not shown in Fig. 3) having two nodes in the AlAs slab.

Coincidentally, an X-like state and the Γ-like bound state meet and mix almost exactly at seven monolayers of AlAs, resulting in the energy shift shown in Fig. 2.

Examination of Fig. 1 shows that the B_2 slab acts as a barrier for electrons near the Γ minimum in the GaAs. It also acts as a well for electron near X minima, although in this case it is bracketed by the deeper but narrow AlAs X-like wells. The X conduction-band edge in the $Al_{0.3}Ga_{0.7}As$ is slightly higher than the $Al_{0.3}Ga_{0.7}As$ Γ minimum (1.751 eV). There are, therefore, a large number of energy states above 1.751 eV as seen in Fig. 2. One set belongs to electrons in the very wide $Al_{0.3}Ga_{0.7}As$ X-like well and the other to near-Γ-minimum electrons with energies higher than the barrier presented by the B_2 slab. Since the eigenvalues of a very wide quantum well are closely spaced, and the parameters of the B_2 slab are fixed, these higher energy eigenvalues are dense and almost independent of the changes in B_1 barrier parameters. Most of these higher energy (>1.751 eV) states are for electrons confined in the B_2 slab, although some derive from mixing of these with states in the other slabs. The number of nodes increases as the energy increases. Two characteristic sets of wave functions can be distinguished by the proportion of anion and cation amplitude. One group of weaker anion amplitude is shown in frames 6, 10, and 12 (1, 2, and 3 nodes, respectively) while stronger anion amplitudes are exhibited by the group in frames 7, 8, 9, and 11 (one to four nodes, respectively). Precisely, each state in the large anion amplitude group is a double state which has two close energy eigenvalues but only one of each double state has been displayed in Fig. 3.

Excited states of electrons confined in the GaAs well are shown in frames 13, 14, and 15 of Fig. 3 at 1.905, 1.916, and 1.919 eV. Comparison of the single node wave functions at 1.582 (frame 1) and 1.916 eV (frame 14) shows the former spreading into the AlAs layer while the latter is more strongly confined. Spreading, through mixing of states in the GaAs and AlAs layers is favored when the proportion of anion amplitude is small. The pair of excited states 1.905 and 1.919 eV both have double nodes in the GaAs slab (frames 13, 15) and show similar preferential spreading at the lower energy. Note that at this stage, it is difficult to identify states in each group which have different proportions of anion and cation amplitude. This is readily clarified, however, from the calculation of dispersion relations described in the following section.

Figure 4 shows the effects of GaAs slab thickness on the energies of zone center states for (001) $Al_{0.3}Ga_{0.7}As/AlAs/GaAs$ DBSL with 2 [Fig. 4(a)] and 7 [Fig. 4(b)] AlAs layers. As in Fig. 1, the GaAs slab is a well for Γ-like electrons and a barrier for X-like electrons. Therefore, when the number of GaAs layers increases, the Γ-like well is widened, the states belonging to electrons in the GaAs Γ-like well are shifted to lower energy while the energies of the electrons in the X-like well should be constant to first order. These differences are generally illustrated in Fig. 4, the almost constant energy state below 1.751 eV, for example, can be identified with an electron in the AlAs X-like well. For less than six GaAs spacer layers, the proximity of left and right AlAs X-like well causes more splitting since the interaction is stronger.

As the width of the GaAs layer is reduced, the energies of Γ-like confined electrons increase, behavior similar to

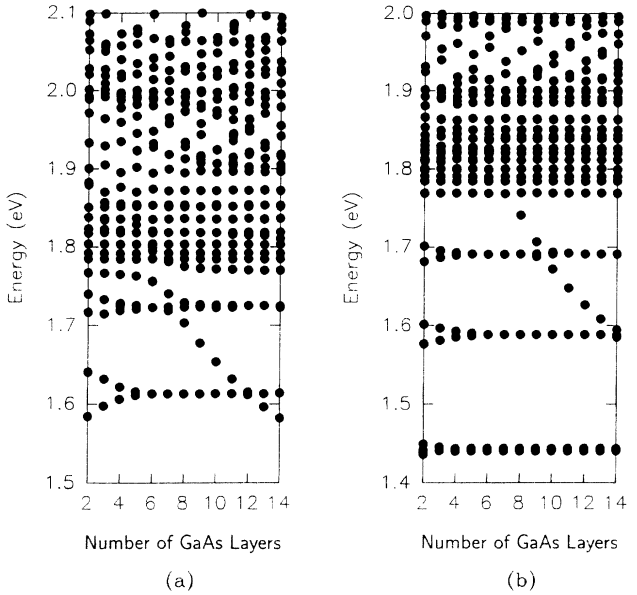

FIG. 4. Electron energy levels at the zone-center state of the (001) $Al_{0.3}Ga_{0.7}As/AlAs/GaAs$ superlattice with (a) two AlAs layers and (b) seven AlAs layers as a function of the number of GaAs layers. The number of $Al_{0.3}Ga_{0.7}As$ layers is 45.

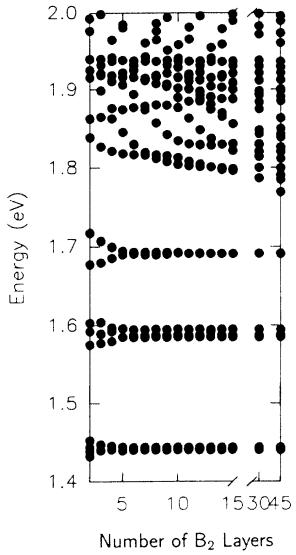

FIG. 5. Electron energy levels at the zone center of the (001) $Al_{0.3}Ga_{0.7}As/AlAs/GaAs$ superlattice as a function of the number of layers in the B_2 barrier slab. There are 14 and seven GaAs and AlAs layers, respectively.

that of the simple GaAs QW with AlAs barrier. An important difference arises when Γ-like and X-like state curves meet. As shown in the study of even parity QW (Ref. 37), the Γ-like and X-like state curves cross if the states have different parities but interact when the parities are the same, giving rise to the Γ-X mixing, anticrossing behavior so the energy is shifted from that predicted by the simple calculation. In addition, with two layers of AlAs, the lowest energy state is from only the Γ-like well if the number of GaAs layers is greater than 12. With seven layers in the B_1 AlAs structure and less than seven GaAs layers, there is no longer a bound Γ-like state. We recall that the eigenenergy of the X-like well is much lower than that of Γ-like well when GaAs and AlAs thickness are equal since the X-like well has a heavier quantization mass.

Figure 5 shows the conduction-band energy levels of zone-center states for $Al_{0.3}Ga_{0.7}As/AlAs/GaAs$ SL with seven layer of AlAs and 14 layer of GaAs calculated as a function of the number of $Al_{0.3}Ga_{0.7}As$ layers. The width of the $Al_{0.3}Ga_{0.7}As$ B_2 barrier principally determines the interaction between SL unit cells. The figure shows that the eigenenergies in the Γ-like and X-like wells in GaAs and AlAs, respectively, are almost constant as the number of B_2 layers is greater than 6. For thinner B_2 layer, the increase in unit-cell interaction become significant and energy splitting occurs. The well states formed by this B_2 slab (states above 1.751 eV) have higher energy and are spaced more widely as the number of B_2 layers decreases.

B. Alloy composition dependence

When the alloy composition is varied, all material parameters, in particular, the energy gap and effective mass, are changed. In the $Al_xGa_{1-x}As$ alloy, the minimum energy gap changes from direct to indirect when $x > 0.45$. We therefore examine the dependence of conduction-band energy levels in (001) $Al_xGa_{1-x}As/Al_yGa_{1-y}As/GaAs$ SL as a function of both alloy composition parameters x and y.

Figures 6(a) and 6(b) show the energies of the zone-center states in a (001) $Al_{0.3}Ga_{0.7}As/Al_yGa_{1-y}As/GaAs$ SL as a function of Al mol fraction (y) in barrier B_1 between 0.3 and 1 for the two and seven layer B_1 structures used previously. The limit $y=1$, corresponds to the AlAs barrier case shown in Fig. 2, while the limit $y=0.3$ has the same structure as the $Al_{0.3}Ga_{0.7}As/GaAs$ single-barrier SL with layer counts (49,14) or (59,14). Both of these have almost the same energy eigenvalues because they have GaAs wells of approximately equal width.

The effect of increasing the Al mol fraction in the B_1 slab is to raise its Γ-like barrier, and lower its X-like well. Knowing this makes it very simple to identify the Γ-like and the X-like states since the energies of the former increase with y while those of the latter decrease. The difference in slopes of the curves can be mainly explained by the difference in the well widths and effective masses. In Fig. 6 it is relatively easy to identify energy states above 1.751 eV as being associated with Γ-like or X-like wells because the increment in the Al composition can be arbitrarily small whereas in Figs. 2, 4, and 5, it is relatively more difficult to identify the shift in individual energy states because atomic layer has to be increased by a minimum of a monolayer at a time.

Considering the two AlAs layer structure [Fig. 6(a)] at composition $y=1$, the 1.582-, 1.769-, 1.810-, 1.900-, and 1.905-eV states have energies which decrease if y is reduced. Thus they correspond with Γ-like states in GaAs or B_2 wells (see frames 1, 6, 10, 12, and 13 in Fig. 3). The 1.810-eV state energy curve has greater slope than the

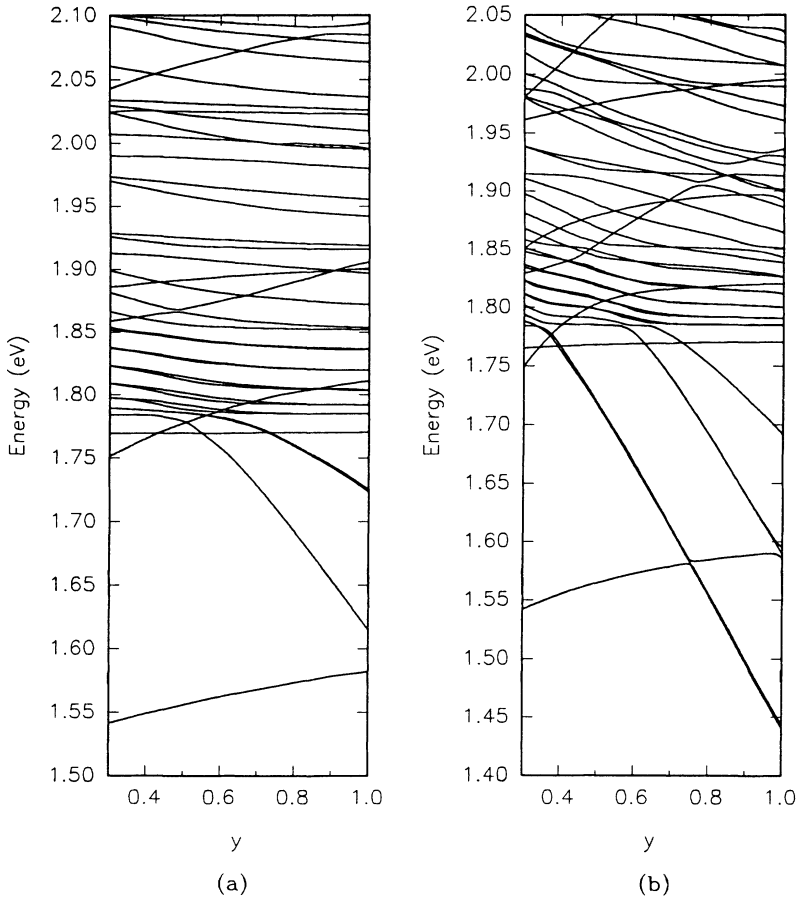

FIG. 6. Electron energy levels at the zone center of the (001) $Al_{0.3}Ga_{0.7}As/Al_yGa_{1-y}As/GaAs$ superlattice with (a) two AlAs layers and (b) seven AlAs layers as a function of Al mol fraction (y) in the B_1 barrier slab. There are 45 and 14 layers of $Al_{0.3}Ga_{0.7}As$ and GaAs, respectively.

other two states, (1.769 and 1.900 eV) in which the electron is confined in the B_2 slab. This can be understood by noting that significant part of the wave function falling in AlAs and GaAs slabs (frame 10 of Fig. 3). Note that the 1.916- and 1.919-eV state wave functions are also confined in GaAs but the energy curve is independent of y composition so they do not behave like Γ-like state and will be further investigated in the next section.

The X-like AlAs confined states (1.613, 1.614, 1.723, and 1.725 eV at $y=1$) have energy rapidly increasing when y decreases, and the bottom of the X-like narrow well rises. The other X-like states confined in the wide B_2 well have almost constant energy because the effect on them of two narrow wells beside the X-like wide B_2 well is very small. The composition dependence in the seven AlAs layer structure [Fig. 6(b)] is similar to that of the two AlAs layer structure, with the addition of two further X-like excited AlAs confined states. It is clearly shown that the ground Γ-like GaAs bound state and the X-like AlAs confined state meet and interact at around 1.590 eV for the $y=1$ structure.

The case where the B_1 barrier composition is fixed at $y=1$ (AlAs) while the Al mol fraction (x) is varied in the barrier B_2 is now considered. The zone-center energy levels for (001) $Al_xGa_{1-x}As/AlAs/GaAs$ SL with two and seven B_1 layers are shown in Figs. 7(a) and 7(b), respectively. The structure with $x=1$ is the same as the (49,14) or (59,14) layer counts of the simple (001) AlAs/GaAs SL with the same energy eigenvalues for Γ-like states. An interesting case is the structure with $x=0$, corresponding to a double-barrier SL structure of (2,14,2) or (7,14,7) AlAs/GaAs/AlAs layers, separated by 45-layer GaAs spacers. The structure with $x=0.3$ is the same as that shown in Fig. 2. The interaction between states can also be noticed as an anticrossing characteristic.

As the Al mol fraction (x) of barrier B_2 increases, the bottom of the wide X-like B_2 well drops, so the energies of densely packed states (i.e., at $x=0.3$, states above 1.751 eV) decrease as x increases. There are a few states with steeply increasing energy when x increases, clearly seen at $x<0.3$ and below the Γ minimum conduction-band-edge energy of the B_2 slab. These states originate from electrons in the Γ-like wells formed by the B_2 slab, the bottom of which raises as x increases. This dependence is quite sensitive and it is therefore easy to distinguish between Γ-like and X-like states. For example for the two AlAs layer structure with $x=0.3$, the 1.769-, 1.810-, and 1.900-eV states trace a steeply increasing curve as X increases, thus they are associated with the Γ-like state. Note that for the two AlAs layer structure when these increasing curves meet other state curves, they are anticrossing only if these states have an even number of nodes in wave function amplitude. The number of nodes in the $x=0.3$ structure at 1.769-, 1.810-, and 1.900-eV states (one to three nodes, frame 6, 10, and 13 in Fig. 3, respectively) can be used to a guide to the number of node in each curve. However, this does not appear in

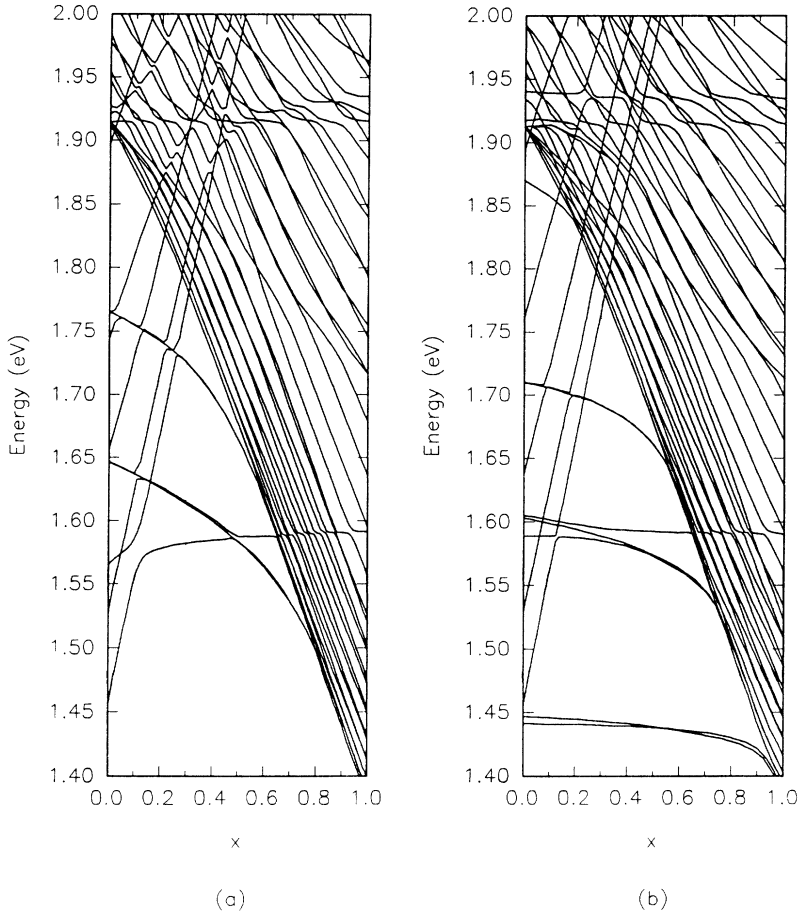

FIG. 7. Electron energy levels at the zone center of the (001) $Al_xGa_{1-x}As/AlAs/GaAs$ superlattice with (a) two AlAs layers and (b) seven AlAs layers as a function of Al mol fraction (x) in the B_2 barrier slab. There are 45 and 14 $Al_xGa_{1-x}As$ and GaAs layers, respectively.

the seven AlAs layer structure [Fig. 7(b)].

In addition to the states in B_2 well, the X-like states bound in AlAs (i.e., 1.613/1.614- and 1.723/1.725-eV states in two AlAs layers with $x=0.3$ structure) decrease in energy as x increases because the barrier height on one side of the AlAs X-like well reduces. The Γ-like bound states in GaAs are almost constant in energy because they mostly depend on the GaAs and AlAs slabs, which are not varied.

For both the two and seven AlAs layer structures, the higher energy trace at around 1.910–1.920 eV is almost constant, in particular, the 1.916-eV state for the two AlAs layer at $x=0.3$, has a large wave function amplitude in the GaAs slab (frame 14, Fig. 3). Thus, this trace belongs to an energy state confined in GaAs which does not depend much on the B_2 slab. There is another parallel constant energy trace in the seven AlAs layer structure [around 1.930–1.940 eV in Fig. 7(b)] which, by noting that the wave function (not shown), has two peaks within the GaAs slab, can be identified as an excited Γ-like state. This is confirmed by the decreasing curve as y decreases in Fig. 6(b) and by the wave vector dependent calculation given in the next section. For the two AlAs layer structure [Fig. 7(a)], the excited Γ-like state in GaAs depends on composition x in the B_2 slab because the electron has a higher probability of tunneling through thin AlAs layers. Thus, not only is there a confined state in the GaAs slab, there is also a slight confinement in the B_2 slab. Consequently, the energy states are shifted due to mixing between B_2 and GaAs confined states.

C. Dependence on wave vector

In the previous two sections, only the electron states at the zone center $\mathbf{k}=0$ and $\mathbf{q}=0$ have been considered. In this section the dependence of the SL energy levels on transverse wave vectors is examined. The energy levels of the (001) $Al_{0.3}Ga_{0.7}As/AlAs/GaAs$ SL with two and seven AlAs layers are plotted in Figs. 8(a) and 8(b), respectively as a function of k_x with k_y and q fixed at 0.

The SL states associated with all three of the X valleys and Γ valley can be distinguished by the characteristics of the curves in Fig. 8. The (100), (010), and (001) X valleys are referred to separately as the X_x, X_y, and X_z respectively. The quantization mass in the (001) SL is the effective mass along [001], equal to the heavier longitudinal mass m_l in the X_z valley and to the lighter transverse mass m_t in both X_y and X_x. In addition the [100] effective mass is accounted for by the dispersion mass along [100], k_x direction, in which m_l is the mass for X_x and m_t for both X_y and X_z valleys.

The X_z and Γ valley states are folded into the region around $k_x=0$, while both the X_x and X_y valley states are folded into the region near $k_x=2\pi/a$.[37] The zone-center towards the left-hand side of Figs. 8(a) and 8(b), identifies the X_z subbands by their smaller curvature due to the

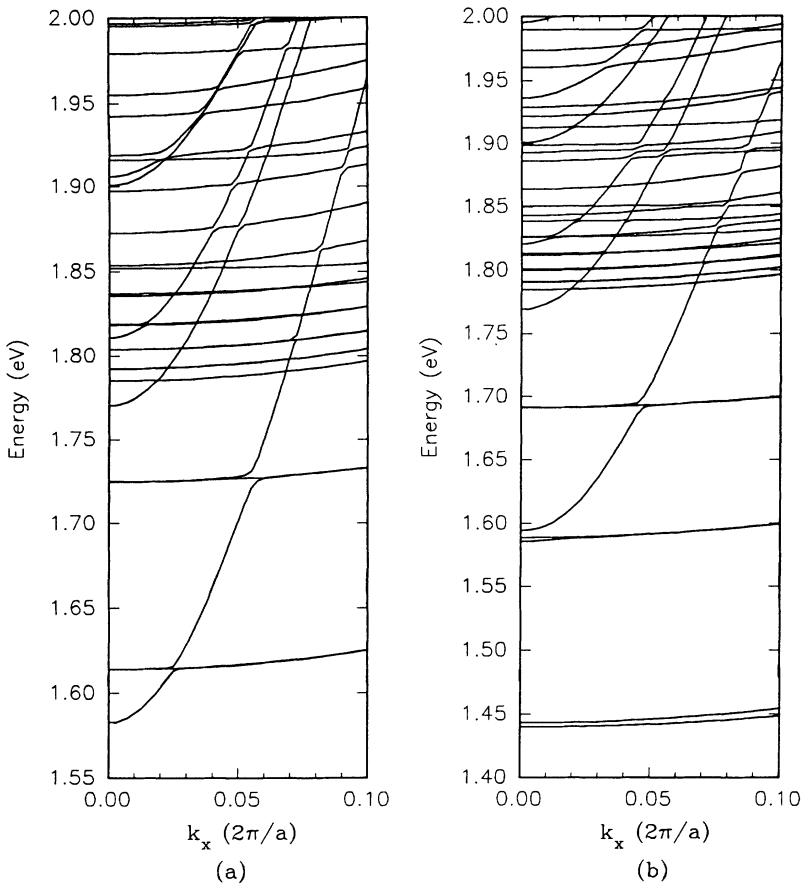

FIG. 8. Electron energy levels of the $\mathbf{q}=0$, $k_y=0$ state for the (001) $Al_{0.3}Ga_{0.7}As$/AlAs/GaAs superlattice with (a) two AlAs layers and (b) seven AlAs layers as a function of k_x. There are 45 and 14 $Al_{0.3}Ga_{0.7}As$ and GaAs layers, respectively.

heavier X_z mass while the larger curvature is associated with the lighter Γ-valley electron.

For structures with two AlAs layers [Fig. 8(a)], the 1.582- and 1.905-eV states at $k_x=0$ have a large curvature and can be identified as ground and first excited Γ-like states confined in the GaAs well (wave function showed in Fig. 3, frame 1 and 13, respectively). The states at 1.916 and 1919 eV, which are also confined in the GaAs well (frames 14 and 15, Fig. 3), can be now identified as a X-like states because of their flat slopes at the left-hand side of Fig. 8(a). These states are unbound states which have energies higher than the barrier of the x-like well (X_c of GaAs = 1.910 eV).

Following Fig. 3, the states confined in the B_2 slab have been separated into two groups by the proportion of anion and cation. The lower anion proportion states (states at 1.769, 1.810, and 1.900 eV in frame 6, 10, and 12, respectively) have large curvature near $k_x=0$ in Fig. 8(a) due to Γ-like states confined in B_2 slab. The other high anion proportion states have small curvatures along k_x and due to their X-like character.

The dispersion relation of the structure with seven AlAs layers as shown in Fig. 8(b) has the same characteristic as the two AlAs layer structure. In both structures the Γ-like state confined in the B_2 slab have about the same energies (three large curvatures at 1.769, 1.810, and 1.900 eV, where $k_x=0$). However, the lowest energy with the large curvature [1.582 and 1.595 eV at $k_x=0$ in Figs. 8(a) and 8(b), respectively] are the Γ-like ground states bound in GaAs and slightly shifted because of additional barrier B_1 as described in Fig. 2. The large curvature of 1.936 eV at the $k_x=0$ state in Fig. 8(b) is a Γ-like excited state confined in GaAs and is equivalent to the large curvature of the state at 1.905 eV at $k_x=0$ in Fig. 8(a). Since the AlAs slab acts as a well for X-like states, the energies of most X-like states, whose dispersion curve are flat, differ between two and seven AlAs layer structures.

IV. SUMMARY

The electron conduction band of the (001) $Al_xGa_{1-x}As/Al_yGa_{1-y}As$/GaAs DBSL has been systematically studied using the semiempirical tight-binding method. It is useful to describe the SL energy states through separate pictures of the conduction-band-edge profiles near Γ minima and near X minima and to explain each in terms of a simple QW model. However when there is a strong interaction among bands or band mixing, the SL energy levels are slightly and exhibit crossing/anticrossing behavior. The mixing of states can also be clearly seen in the wave-function amplitudes.

The electron energy levels as functions of thickness of each slab in (001) $Al_{0.3}Ga_{0.7}As$/AlAs/GaAs DBSL have been examined individually, the results show the effect of well and barrier width for electron near both Γ and X minima and show the interaction between wells when

spacer thickness is reduced. With regard to the results of the energy as a function of an additional barrier (AlAs slab) thickness, the energy levels of electron near Γ minima has value approximately equal to that in a case of simple AlAs/GaAs SL when there are more than four AlAs layers. This has a major role in QWIP. The results also show that there are X-like states in which electron are confined in the AlAs slab. These X-like states are a double state due to symmetric and asymmetric eigenfunctions of the double X-like wells. As the result of the dependence of X-like well width, the state energy decreases when the AlAs layer is thickened. However, these coupled states clearly split in energy when the two X-like wells (AlAs) become closer. In the GaAs thickness dependence calculation, the Γ-like bound-state energies are found to decrease and the X-like state energies remain approximately constant when GaAs layer thickness is increased. Above 1.751 eV there are dense states which mostly originate from electrons near both Γ and X minima confined in the wide $Al_{0.3}Ga_{0.7}As$ slab.

The eigenenergy dependence on x and y alloy composition for (001) $Al_xGa_{1-x}As/Al_yGa_{1-y}As/GaAs$ DBSL is a main consequence of the Γ-like and X-like well barrier height variation. When Al mol fraction (y) in the additional barrier B_1 increases, the Γ-like GaAs well barrier height is raise so that the Γ-like state energies are increased. Simultaneously, the depth of X-like AlAs well is increased so the X-like bound-state energies are decreased. Moreover, when the outer barrier Al mol fraction (x) increases, the barrier height of the Γ-like GaAs well remains constant but the lowest energy of the Γ-like B_2 well rises, so the energy of set of Γ-like bound states in GaAs is constant and while that of the set bound in B_2 steeply increases. The energies of X-like state in narrow B_1 decrease slightly as x increases because well becomes deeper. In the wide B_2 wells, the energies of the X-like states steeply decrease as x increases because the bottoms of these wells are lowered. Since x and y are continuous by variable parameters, it is relatively easy to identify energy states and the composition at which they meet, the anticrossing and crossing behaviors are readily seen.

The energy dispersive relation for (001) $Al_{0.3}Ga_{0.7}As/AlAs/GaAs$ DBSL along the wave vector parallel to the interface illustrates the different curvatures due to the different effective masses. The dispersion curve of Γ-like states near the zone-center has a larger curvature than that of the X-like state because of the lighter Γ-valley electron mass. This allows states to be identified as Γ-like or X-like by the effective mass characteristic rather than by the slab in which the electron is confined. For example, in the two AlAs layer structure, the 1.916- and 1.919-eV states are confined in the GaAs slab but their dispersion curves are flat, in other words their effective masses are large so they can be identified as a X-like states.

In order to compared our results with the EFM method described in the introduction we have recalculated the energy states using the same parameters (conduction-band edge and effective mass) at the Γ point. In a parabolic band approximation, the ground and first excited state energies of a two layer AlAs structure are 1.563 and 2.026 eV, compared with the tight-binding result of 1.582 and 1.905 eV, respectively. The first excited state shows a greater energy difference because of nonparabolic effects. When the nonparabolicity parameter, $\alpha=0.7$ (Ref. 38) is applied to both the barriers and well materials, the first excited state become closer at 1.899 eV while the ground state is reduced to 1.522 eV. The ground state in this structure is thus most affected by the nonparabolic band because of the high AlAs barrier (1.072 eV). Since this structure has high-energy states and very large potential energy, SL states are not well described by the EFM method using parameters at the symmetry points only.

As an example of the genre, a typical structure with 45 layers of $Al_{0.3}Ga_{0.7}As$, two layers of AlAs, 14 layers of GaAs, and then two layers of AlAs was studied. It has Γ-like bound and first excited quasibound states at 1.582 and 1.905 eV, respectively. This corresponds to 323 meV energy difference which it is suitable for 3–5 μm QWIP application. The addition of thin AlAs slabs has a small effect on response energy for the Γ-like state. In addition, as the AlAs thickness increases, the X-like state has lower energy and can become the lowest state, which will cause some perturbation to the response energy. The response energy can most readily be adjusted by the thickness of the GaAs slab, although a thin GaAs slab may raise the Γ-like state energy above that of the X-like state the structure acts as a SL type-II rather like the short-period simple SL case.

[1]B. F. Levine, J. Appl. Phys. **74**, R1 (1993).
[2]B. F. Levine, Semicond. Sci. Technol. **8**, S400 (1993).
[3]B. F. Levine, K. K. Choi, C. G. Bethea, J. Walker, and R. J. Malik, Appl. Phys. Lett. **50**, 1092 (1987).
[4]A. Koch, E. Gornik, G. Abstreiter, G. Bohm, M. Walther, and G. Weimann, Appl. Phys. Lett. **60**, 2011 (1992).
[5]K. Kheng, M. Ramsteiner, H. Schneider, J. D. Ralston, F. Fuchs, and P. Koidl, Appl. Phys. Lett. **61**, 666 (1992).
[6]B. F. Levine, G. Hasnain, C. G. Bethea, and N. Chand, Appl. Phys. Lett. **54**, 2704 (1989).
[7]B. F. Levine, C. G. Bethea, K. K. Choi, J. Walker, and R. J. Malik, J. Appl. Phys. **64**, 159 (1988).
[8]S. S. Li, M. Y. Chuang, and L. S. Yu, Semicond. Sci. Technol. **8**, S406 (1993).
[9]K. K. Choi, L. Fotiadis, M. Taysing-Lara, W. Chang, and G. J. Lafrate, Appl. Phys. Lett. **60**, 592 (1992).
[10]H. Schneider, P. Koidl, F. Fuchs, B. Dischler, K. Schwarz, and J. D. Ralston, Semicond. Sci. Technol. **6**, C121 (1991).
[11]H. Schneider, F. Fuchs, B. Dischler, J. D. Ralston, and P. Koidl, Appl. Phys. Lett. **58**, 2234 (1991).
[12]M. S. Kiledijian, J. N. Schulman, and K. L. Wang, Surf. Sci. **267**, 454 (1992).
[13]M. S. Kiledjian, J. N. Schulman, and K. L. Wang, Phys. Rev. B **44**, 11, 5616 (1991).
[14]B. F. Levine, A. Y. Cho, J. Walker, R. J. Malik, D. A. Kleinman, and D. L. Sivco, Appl. Phys. Lett. **52**, 1481 (1988).

[15]G. Neu, Y. Chen, C. Deparis, and J. Massies, Appl. Phys. Lett. **58**, 2111 (1991).
[16]Y. Chen, G. Neu, C. Deparis, and J. Massies, Proc. SPIE **1361**, 860 (1990).
[17]J. N. Schulman and Y.-C. Chang, Phys. Rev. B **31**, 2056 (1985).
[18]D. J. Wolford, T. F. Kuech, and J. A. Bradley, J. Vac. Sci. Technol. B **4**, 1043 (1986).
[19]G. Danan, B. Etienne, F. Mollot, and R. Planel, Phys. Rev. B **35**, 6207 (1987).
[20]J. Menendez, A. Pinczuk, D. J. Werder A. C. Gossard, and J. H. English, Phys. Rev. B **33**, 8863 (1986).
[21]U. Venkateswaran, M. Chandrasekhar, and H. R. Chandrasekhar, Phys. Rev. B **33**, 8416 (1986).
[22]L. Hrivnak, Appl. Phys. Lett. **56**, 2425 (1990).
[23]P. Dawson, Opt. Quantum Electron. **22**, S231 (1990).
[24]M. Leroux, N. Grandjean, B. Chastaingt, C. Deparis, G. Neu, and J. Massies, Phys. Rev. B **45**, 20, 11 846 (1992).
[25]G. Bastard, *Wave Mechanics Applied to Semiconductor Heterostructures* (Halsted, New York, 1988).
[26]M. C. Munoz, V. R. Velasco, and F. Garcia-Moliner, Phys. Rev. B **39**, 1786 (1989).
[27]Y. Lu and L. J. Sham, Phys. Rev. **40**, 5567 (1989).
[28]L. Brey and C. Tejedor, Phys. Rev. **35**, 9112 (1981).
[29]K. Oda and T. Nakayama, Jpn. J. Appl. Phys. **31**, 2359 (1992).
[30]M. Morifuji, Y. Nishikawa, C. Hamaguchi, and T. Fujii, Semicond. Sci. Technol. **7**, 1047 (1992).
[31]J. Arriaga, M. C. Munoz, V. R. Velasco, and F. Garcia-Molinear, Phys. Rev. B **43**, 9626 (1991).
[32]J. B. Xia, S. F. Ren, and Y. C. Chang, Phys. Rev. B **43**, 1692 (1991).
[33]D. J. Chadi and M. L. Cohen, Phys. Status Solidi B **68**, 405 (1975).
[34]G. Platero, J. Sanchez-Dehesa, C. Tejedor, and F. Flores, Surf. Sci. **168**, 553 (1986).
[35]Y. Fu and K. A. Chao, Phys. Rev. B **43**, 4119 (1991).
[36]J. N. Schulnam and T. C. McGill, Phys. Rev. **19**, 6341 (1979).
[37]D. Z.-Y. Ting and Y.-C. Chang, Phys. Rev. B **36**, 4359 (1987).
[38]J. A. Lopez-Villanueva, I. Melchor, P. Cartujo, and J. E. Carceller, Phys. Rev. B **48**, 1626 (1993).